Final Project for *8.334: Statistical Physics of Fields*
Primary authors: **Ming Zheng. Physics**
Correspond to smile321@mit.edu

RNA MEDIATES THE PHYSICAL BIOLOGY OF PHASE-SEPARATED TRANSCRIPTIONAL CONDENSATES

(Dated: May 22, 2021)

Recent studies demonstrated that transcriptional proteins could functionalize as liquid-liquid phase-separated (LLPS) condensates. However, how RNA dynamics are coupled to such LLPS condensates are largely unknown. In this work, I used field approach to study the phase-separation behaviors of transcriptional condensates relating to RNA-protein interactions. In the equilibrium limit, I found the increased length of RNA can "buffer" the transcriptional proteins and result in reduced condensate size; I also found the relative strength between self and mutual interactions of proteins and RNAs at critical point determines whether the system undergoes a phase-transition into a mixed or a demixed phase; Renormalization group analysis unveils the mutual interaction as a non-irrelevant component, which indicates the importance of RNA-protein interaction in determining the critical phase-transition behavior. In the non-equilibrium limit, I found nascent transcription could be crucial to stabilize the nucleation process of transcriptional condensates. *In situ* degradation/trimming of overlong RNAs into small pieces can fasten the nucleation. I also built up the framework regarding the perturbative RG of Gaussian model as well as the dynamical interactions between enhancer and promoter (gene). Most theoretical and simulation discoveries are consistent with experiments.

INTRODUCTION

Cells form biomolecular condensates to compartmentalize and concentrate biochemical reactions (e.g.: nucleoli, stress granules, etc.) [1]. Recent studies demonstrate that transcriptional proteins also form condensates that are liquid-liquid phase-separated (LLPS) inside nuclei and cumulate at super-enhancers (SEs) [2, 3]. These transcriptional proteins typically have an intrinsically disordered region (IDR) that forms unstructured random coils thus facilitates condensation by nanoscale weak multivalent interactions, and such IDRs form LLPS droplets on their own in vitro [4]. However, IDR-mediated condensation of biomolecules is a self-enhanced, one-way process, which cannot explain the finite lifetime for most transcriptional clusters [5] and gene burst duration [6]. A recent research from Richard Young Lab found in vitro evidence of a charge-balance between the negative-charged RNAs and the positive-charged transcriptional proteins (TPs): moderate RNA concentration promotes the condensation of TPs while over-high concentration dissolves such condensates [7]. Another work from Anthony Hyman Lab also indicates that RNA buffers the phase separation behavior of prion-like RNA binding proteins, such as FUS, TDP43, and hnRNPA1 [8]. Therefore, RNA could potentially be an important participant in tuning the equilibrium and dynamics of transcriptional condensates.

RNA has at least three features that could interact with proteins: 1. Sequence-specific motifs that directly bind with RNA-recognition proteins; 2. net negative charges which are proportional to the number of phosphate groups (i.e., number of base-pairs); 3. RNA-secondary structures that result in either compact or more swollen structures (due to differential fraction of bound pairs), where the latter case physically exclude proteins nearby (FIG. 1). As for transcriptional proteins, previous works demonstrated that can LLPS by their own *in vitro* due to the fact that many of them (like Mediator, BRD4, RNAP II CTD) have IDRs, which promote phase transition from dilute phase into a condensed phase through weak multivalent interactions independent of RNAs. Based on these features of RNAs and transcriptional proteins, we can write down the energy density in the field representation with the field of protein $\phi_p(\mathbf{x})$ and the field of RNA $\phi_r(\mathbf{x})$:

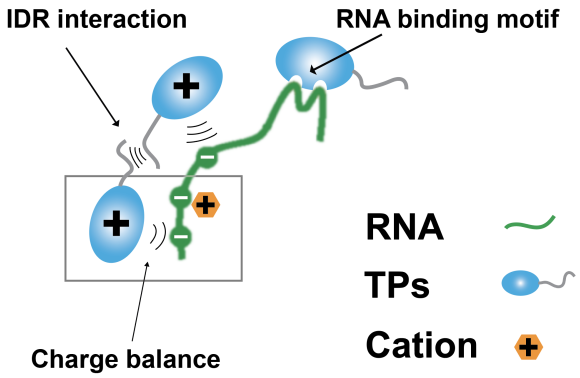

FIG. 1: Interactions involved in RNA-protein solution.

$$\beta\Psi\left[\phi_p(\mathbf{x}),\phi_r(\mathbf{x})\right] = \frac{1}{2}\phi_p^2(\phi_p-1)^2 + \frac{K}{2}|\nabla\phi_p|^2 + \frac{L}{2}|\nabla^2\phi_p|^2 + \frac{1}{2}\phi_r^2 - M\phi_p\phi_r + \frac{E}{2}(\phi_p-\rho\phi_r)^2 + S\phi_r^4 + W\phi_p^2\phi_r^2. \quad (1)$$

The first term is a double-well potential, which captures the IDR-interaction of proteins on their own. K and L capture the surface tension of protein droplets to the lowest order. M stands for the mutual interaction between RNA and protein to the lowest order (the law of mass action). E is the coefficient confining the electrostatic balance of RNA and protein to the lowest order. ρ is the relative charge of each RNA to protein molecule, and should be proportional to the RNA length. S and W are the next lowest-order penalty factors that constrain the saturation volume of RNA and protein within each voxel. More details about the derivation of Eq. 1 can be found in Supplements.

Based on Eq. 1, we can further extend this model to study the contexts of equilibrium as well as the non-equilibrium, accordingly.

THERMODYNAMIC NUCLEATION OF TRANSCRIPTIONAL CONDENSATES GOVERNED BY FIRST ORDER PHASE TRANSITION

If we assume the densities of protein and RNA inside a condensate are roughly uniform, we can write down the total energy of a condensate incorporating n_p number of protein molecules and n_r number of RNA molecules as

$$E_C(n_p,n_r) = a(n_p+\upsilon n_r)^{2/3} - bn_p + c(n_p-\rho n_r)^2. \quad (2)$$

In this expression, the total volume of a condensate is proportional to the total molecules inside, where υ is a correction factor that describes the relative volume of a RNA compared with that of a protein ($\upsilon \propto \rho^{1.5}$ under the assumption that RNA is a fluctuating polymer with a definite persistence length); thus, $(n_p+\upsilon n_r)^{2/3}$ scales with the total surface area. a is the surface-tension energy coefficient, which is equivalent to the penalty factors K and L in Eq. 1. b is the relative bulk energy gain due to the protein-protein multivalency interactions in the condensed phase compared with the dilute phase. This parameter can be either positive or negative, decided by the relative chemical potential of the condensed phase [9]:

$$b = \Delta\mu = k_BT\log\left(\frac{c_{\text{dil}}}{c_{\text{sat}}}\right), \quad (3)$$

where c_{dil} is the ambient protein concentration in the dilute phase and c_{sat} is the saturation concentration dependent on the nature of IDR interaction. When b switches from negative to positive, the energy landscape undergoes a 1st-order phase transition, where a coarsening basin appears at infinity (FIG. 2). c is the parameter constraining the overall protein-RNA charge balance, which is equivalent to E in Eq. 1. ρ again is the relative charge of a RNA molecule to a protein molecule.

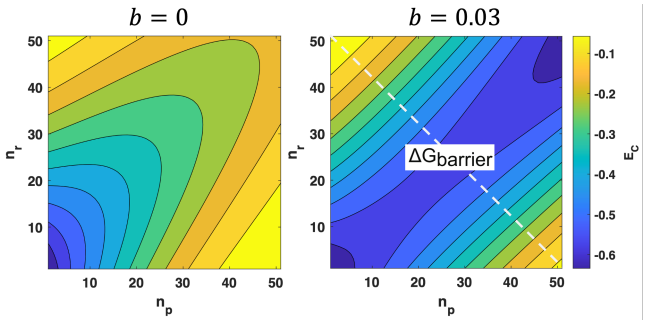

FIG. 2: Free energy landscape before/after supersaturation. $\rho = 1$, $a = 0.1$, and $c = 0.001$ are applied in Eq. 2.

Beyond supersaturation, when a total of Λ nucleation sites present in a canonical ensemble, the partition function of N_p protein molecules and N_r RNA molecules can be written as:

$$Z(N_p,N_r) = \sum_{\{n_p,n_r\}} p(n_p^0,n_r^0)\times e^{-\beta\sum_s' E_C(n_p^s,n_r^s)}. \quad (4)$$

$p(n_p^0,n_r^0)$ represents the likelihood of having n_p^0 protein molecules and n_r^0 RNA molecules in the dilute (ambient) phase. The comma $'$ on the summation indicates the total number of protein and RNA molecules from different condensates "s" are constrained by $(N_p-n_p^0)$ and $(N_r-n_r^0)$, respectively. This partition function is hard to solve; fortunately, after introducing two fugacities w and z for protein and RNA, respectively, we can convert the partition in Eq. 4 to a grand partition function:

$$\Xi(w,z) = \Big(\sum_{n_p,n_r} w^{n_p}z^{n_r}e^{-\beta E_C(n_p,n_r)}\Big)^{\Lambda}. \quad (5)$$

Now we can sum over the $\{n_p,n_r\}$ independently without any constraint for all the Λ nucleation sites. Accordingly, we can easily derive the thermodynamic free energy, total number of molecules in condensed phase, as well as the molecule number fluctuation of each condensate:

$$\mathcal{F} = -k_BT\log\Xi, \quad (6)$$

$$\langle N_p\rangle = w\frac{\partial}{\partial w}\log\Xi, \quad \langle N_r\rangle = z\frac{\partial}{\partial z}\log\Xi, \quad (7)$$

$$\langle(n-\langle n\rangle)^2\rangle = \frac{1}{\Lambda}\big[y\frac{\partial}{\partial y}\log\Xi + y^2\frac{\partial^2}{\partial y^2}\log\Xi\big], \quad (8)$$

where $y\mapsto w$ for $\langle(\Delta n_p)^2\rangle$ and $y\mapsto z$ for $\langle(\Delta n_r)^2\rangle$, and $\langle n\rangle$ is simply $\langle N\rangle/\Lambda$. More details about deriving the grand partition function and corresponding derivatives can be found in Supplements.

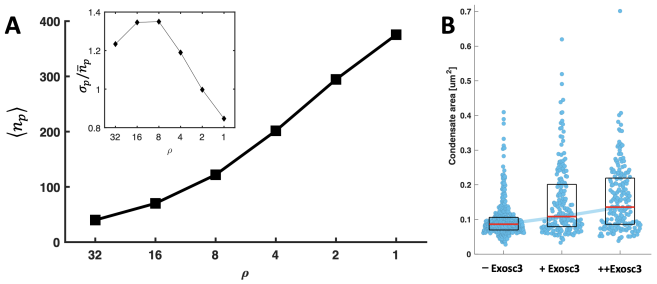

FIG. 3: Relationship between net charge per RNA and condensate size. (A) Theoretical calculation of protein molecules per condensate with various RNA charge. Eq. 7 and 8 are used to calculate $\langle n_p \rangle$ and σ_p^2, respectively. $w = 0.99$, $z = 1 - (1/(1-w)/\rho)^{-1}$, $v = (\rho/2)^{1.5}$, $a = 0.1$, $b = 0.03$, and $c = 0.001$ are applied for Ξ. (B) Experimental Mediator condensate size upon differential Exosc3 level. *Med19* in mouse stem cells was labeled with Halo-JF549 dye and proceed to fluorescent microscope imaging.

Based on the grand partition function, we can study the influence of the charge of RNA upon the size of transcriptional condensates. In FIG. 3A, the average number of protein molecules per condensate is calculated via Eq. 7 with differential ρ value. As we can see, as the net charge (i.e., RNA length) drops, condensates are growing bigger. To experimentally capture this phenomenon, I engineered a cell line that can express tunable amount of Exosc3, which is a major component of the RNA Exosome complex. RNA Exosome can trim and degrade RNAs to small pieces [10]; therefore, by expressing more and more Exosc3, I'm effectively tuning down the RNA length (i.e. net negative charge per RNA, ρ) inside a cell. In FIG. 3B, I chose Mediator as the transcriptional protein of interest and treated cells with increasing amount of Exosc3. As the analysis shown from experimental data, Mediator condensate size increases upon tuning down the RNA length, which is consistent with the calculation from the grand partition function.

LANDAU-GINZBURG EXPANSION AROUND CRITICAL POINT

In this section, I'm going to perform Landau-Ginzburg expansion upon Eq. 1 around critical point. Accordingly, we can analyze the bifurcation behavior based on saddle point approximation; moreover, we can further perform renormalization group to study the critical behavior.

Saddle Point Approximation

At critical point, the partition function is

$$\begin{aligned} Z &= \int \mathcal{D}\phi_p(\mathbf{x})\mathcal{D}\phi_r(\mathbf{x})\, \exp\big\{-\beta\mathcal{H}[\phi_p(\mathbf{x}),\phi_r(\mathbf{x})]\big\} \\ &= \int \mathcal{D}\phi_p(\mathbf{x})\mathcal{D}\phi_r(\mathbf{x})\, \exp\Big\{-\int d^d\mathbf{x}\,\hat{\Psi}\Big\}, \end{aligned} \tag{9}$$

where the energy density $\hat{\Psi}$ is expanded in the Landau-Ginzburg convention:

$$\begin{aligned} &\hat{\Psi}[\phi_p(\mathbf{x}),\phi_r(\mathbf{x}),\nabla\phi_p,\nabla^2\phi_p] \\ =\ & \frac{t}{2}\phi_p^2 + \frac{K}{2}|\nabla\phi_p|^2 + \frac{L}{2}|\nabla^2\phi_p|^2 + \frac{s}{2}\phi_r^2 \\ -\ & m\phi_p\phi_r + u\phi_p^4 + v\phi_r^4 + w\phi_p^2\phi_r^2. \end{aligned} \tag{10}$$

For the reason of charge conjugation symmetry, ($\mathcal{H}$ should remain unchanged after $\phi_{p,r} \mapsto -\phi_{p,r}$), only even-order terms are kept. Assume the configuration with the maximum probability is a uniform solution, which dominates the free energy:

$$\beta F = -\log Z = V \min_{(\bar{\phi}_p,\bar{\phi}_r)} \hat{\Psi}_0[\bar{\phi}_p,\bar{\phi}_r]. \tag{11}$$

Explicitly, the mean field solution is

$$\begin{aligned} \frac{\partial\hat{\Psi}_0}{\partial\bar{\phi}_p} &= t\bar{\phi}_p - m\bar{\phi}_r + 4u\bar{\phi}_p^3 + 2w\bar{\phi}_r^2\bar{\phi}_p = 0, \\ \frac{\partial\hat{\Psi}_0}{\partial\bar{\phi}_r} &= s\bar{\phi}_r - m\bar{\phi}_p + 4v\bar{\phi}_r^3 + 2w\bar{\phi}_p^2\bar{\phi}_r = 0. \end{aligned} \tag{12}$$

Eq. 12 are indeed two smooth plane curves in a real Euclidean plane $\mathbb{R}^2$ with degree of 3, and the solutions are where tangency or intersections happen. For simplicity, let's focus on a symmetric case, where $t = s$ and $u = v$. Furthermore, let's normalize all factors by $4u$ (since u is always positive), i.e. $\tilde{t} = t/4u$, $\tilde{m} = m/4u$, and $\tilde{w} = 2w/4u$. In this special case, we can recombine Eq. 12 to get the following equations:

$$\begin{aligned} \tilde{t}(\bar{\phi}_p+\bar{\phi}_r) &- \tilde{m}(\bar{\phi}_p+\bar{\phi}_r) \\ &+ \bar{\phi}_p^3 + \bar{\phi}_r^3 + \tilde{w}(\bar{\phi}_r^2\bar{\phi}_p + \bar{\phi}_r\bar{\phi}_p^2) = 0, \\ \tilde{t}(\bar{\phi}_p-\bar{\phi}_r) &+ \tilde{m}(\bar{\phi}_p-\bar{\phi}_r) \\ &+ \bar{\phi}_p^3 - \bar{\phi}_r^3 + \tilde{w}(\bar{\phi}_r^2\bar{\phi}_p - \bar{\phi}_r\bar{\phi}_p^2) = 0. \end{aligned} \tag{13}$$

These two equations can be further rearranged to

$$\begin{aligned} &(\bar{\phi}_p+\bar{\phi}_r)\cdot(\tilde{t}-\tilde{m}+\bar{\phi}_p^2-\bar{\phi}_p\bar{\phi}_r+\bar{\phi}_r^2+\tilde{w}\bar{\phi}_p\bar{\phi}_r) = 0, \\ &(\bar{\phi}_p-\bar{\phi}_r)\cdot(\tilde{t}+\tilde{m}+\bar{\phi}_p^2+\bar{\phi}_p\bar{\phi}_r+\bar{\phi}_r^2-\tilde{w}\bar{\phi}_p\bar{\phi}_r) = 0. \end{aligned} \tag{14}$$

The solution of a disordered phase can be immediately recognized:

$$\begin{cases} \bar{\phi}_p+\bar{\phi}_r = 0, \\ \bar{\phi}_p-\bar{\phi}_r = 0. \end{cases} \quad\Rightarrow\quad \bar{\phi}_p = \bar{\phi}_r = 0. \tag{15}$$

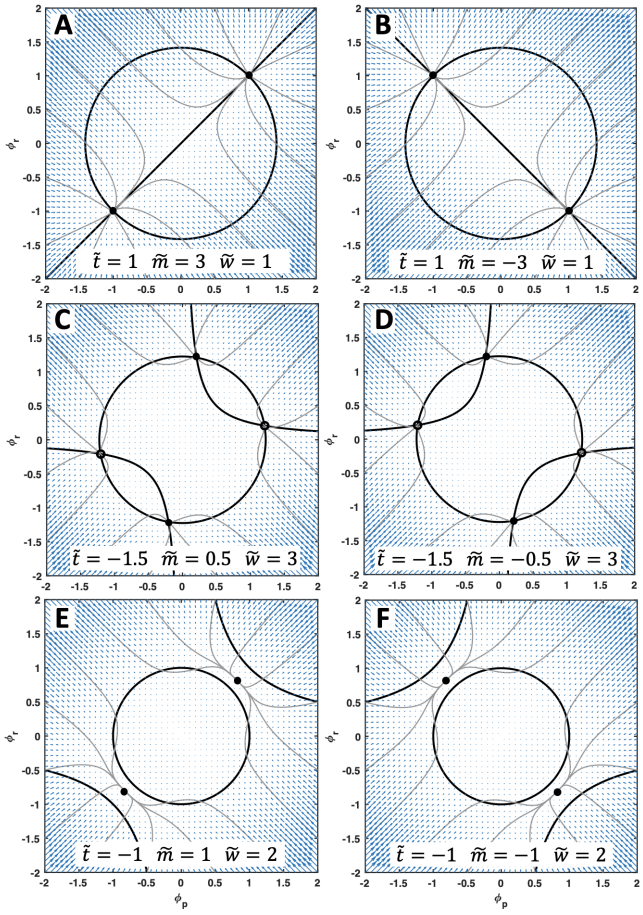

FIG. 4: Fixed points from saddle point approximation in different cases.

The stability of the disordered phase can be obtained by calculating the eigenvalues of the Hessian matrix at this point:

$$\mathbf{H} = \begin{pmatrix} \tilde{t}+3\bar{\phi}_p^2+\tilde{w}\bar{\phi}_r^2, & -\tilde{m}+2\tilde{w}\bar{\phi}_r\bar{\phi}_p \\ -\tilde{m}+2\tilde{w}\bar{\phi}_p\bar{\phi}_r, & \tilde{t}+3\bar{\phi}_r^2+\tilde{w}\bar{\phi}_p^2 \end{pmatrix}_{\bar{\phi}_p,\bar{\phi}_r=0} = \begin{pmatrix} \tilde{t} & -\tilde{m} \\ -\tilde{m} & \tilde{t} \end{pmatrix}. \tag{16}$$

Solving the corresponding eigen-determinant yields

$$\lambda^2 - 2\tilde{t}\lambda + \tilde{t}^2 - \tilde{m}^2 = 0; \tag{17}$$

$$\Rightarrow \quad \lambda_1+\lambda_2 = 2\tilde{t},\ \lambda_1\lambda_2 = \tilde{t}^2-\tilde{m}^2. \tag{18}$$

When (i) $\tilde{t}>0$ and (ii) $|\tilde{t}|>|\tilde{m}|$, the disordered phase is stable. Once any one of these two conditions is disobeyed, the system goes under phase transition.

A non-trivial solution of Eq. 14 yields:

$$\begin{cases} \tilde{t}-\tilde{m}+\bar{\phi}_p^2-\bar{\phi}_p\bar{\phi}_r+\bar{\phi}_r^2+\tilde{w}\bar{\phi}_p\bar{\phi}_r=0, \\ \bar{\phi}_p-\bar{\phi}_r=0. \end{cases} \tag{19}$$

$$\Rightarrow \quad \bar{\phi}_p=\bar{\phi}_r=\pm\sqrt{\frac{\tilde{m}-\tilde{t}}{1+\tilde{w}}}. \tag{20}$$

Obviously, this case is valid only when $\tilde{m}>\tilde{t}$. This is an attractive-interaction dominated phase transition, where one condensed phase enriched as a mixture of both protein and RNA molecules, coexisting with a diluted phase depleted in both components (FIG. 4A).

Another non-trivial solution of Eq. 14 yields:

$$\begin{cases} \bar{\phi}_p+\bar{\phi}_r=0, \\ \tilde{t}+\tilde{m}+\bar{\phi}_p^2+\bar{\phi}_p\bar{\phi}_r+\bar{\phi}_r^2-\tilde{w}\bar{\phi}_p\bar{\phi}_r=0. \end{cases} \tag{21}$$

$$\Rightarrow \quad \bar{\phi}_p=-\bar{\phi}_r=\pm\sqrt{\frac{-\tilde{m}-\tilde{t}}{1+\tilde{w}}}. \tag{22}$$

Obviously, this case is valid only when $-\tilde{m}>\tilde{t}$. This is a repulsive-interaction dominated phase transition, where two components are demixed: one phase is enriched in protein molecules, while the other phase is enriched in RNA molecules (FIG. 4B).

There is a third non-trivial solution from Eq. 14:

$$\begin{cases} \tilde{t}-\tilde{m}+\bar{\phi}_p^2-\bar{\phi}_p\bar{\phi}_r+\bar{\phi}_r^2+\tilde{w}\bar{\phi}_p\bar{\phi}_r=0, \\ \tilde{t}+\tilde{m}+\bar{\phi}_p^2+\bar{\phi}_p\bar{\phi}_r+\bar{\phi}_r^2-\tilde{w}\bar{\phi}_p\bar{\phi}_r=0. \end{cases} \tag{23}$$

$$\Rightarrow \quad \bar{\phi}_p^2+\bar{\phi}_r^2=-\tilde{t},\ \ \bar{\phi}_p\bar{\phi}_r=\frac{\tilde{m}}{\tilde{w}-1}. \tag{24}$$

The leftside equation in Eq. 24 is a circle, and the rightside one is an inverse-proportional function. When $\left|\frac{\tilde{m}}{\tilde{w}-1}\right| < -\frac{\tilde{t}}{2}$, the inverse-proportional function have four intersections with the circle. Since $t<0$ for sure, both protein and RNA molecules behave like self-attracting particles. When $\frac{\tilde{m}}{\tilde{w}-1}>0$, there is a competition between homogeneous and heterogeneous attraction, which results in two pairs of "skewed" mixing phases (FIG. 4C). When $\frac{\tilde{m}}{\tilde{w}-1}<0$, there is a hybrid effect of self-attraction and mutual-repulsion, which results in two pairs of "skewed" demixed phases (FIG. 4D).

When keeping on increasing $|m|$ till $\left|\frac{\tilde{m}}{\tilde{w}-1}\right| > -\frac{\tilde{t}}{2} > 0$, there seem to be only spiral solutions available from Eq. 24. Actually, a fork bifurcation happened and two stable fixed points merge into one point either along $\bar{\phi}_p=\bar{\phi}_r$ or along $\bar{\phi}_p=-\bar{\phi}_r$ (for $m>0$ or $m<0$, respectively). In this case, either Eq. 19 or 21 will take over the solutions of fixed points again, indeed (FIG. 4E,F).

After combing all cases, we can draw the full phase diagram around the critical point, as shown in FIG. 5.

Renormalization group under scaling hypothesis

The renormalization group (RG) of the Gaussian model is most conveniently performed in terms of the

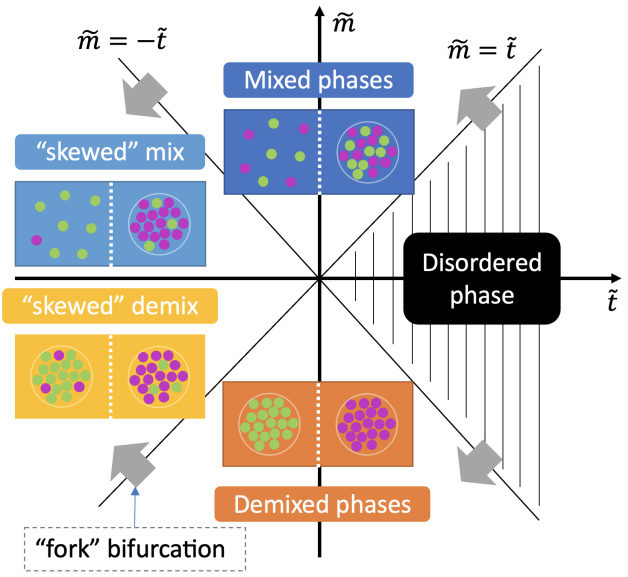

FIG. 5: The full phase diagram under saddle point approximation. $\tilde{w} = 3$ for convenience.

Fourier modes:

$$\begin{aligned} Z &= \int \mathcal{D}\phi_p(\mathbf{q})\mathcal{D}\phi_r(\mathbf{q})\, e^{-\beta\mathcal{H}_0-\mathcal{U}} \\ &= \int \mathcal{D}\phi_p(\mathbf{q})\mathcal{D}\phi_r(\mathbf{q})\, \exp\Big\{-\int_0^\Lambda \frac{d^d\mathbf{q}}{(2\pi)^d}\times \\ &\quad \Big[\frac{t+Kq^2+Lq^4}{2}|\phi_p(\mathbf{q})|^2+\frac{s}{2}|\phi_r(\mathbf{q})|^2 \\ &\quad -m\phi_p(\mathbf{q})\phi_r(-\mathbf{q})\Big]\Big\}\times e^{-\mathcal{U}}, \end{aligned} \tag{25}$$

where $\Lambda = \pi/a$ (a is the block size), and

$$\begin{aligned} \mathcal{U} &= \int_0^\Lambda \frac{d^d\mathbf{q_1}d^d\mathbf{q_2}d^d\mathbf{q_3}}{(2\pi)^{3d}}\times \\ &\quad \Big[u\cdot\phi_p(\mathbf{q_1})\phi_p(\mathbf{q_2})\phi_p(\mathbf{q_3})\phi_p(-\mathbf{q_1}-\mathbf{q_2}-\mathbf{q_3}) \\ &+ v\cdot\phi_r(\mathbf{q_1})\phi_r(\mathbf{q_2})\phi_r(\mathbf{q_3})\phi_r(-\mathbf{q_1}-\mathbf{q_2}-\mathbf{q_3}) \\ &+ w\cdot\phi_p(\mathbf{q_1})\phi_p(\mathbf{q_2})\phi_r(\mathbf{q_3})\phi_r(-\mathbf{q_1}-\mathbf{q_2}-\mathbf{q_3})\Big]. \end{aligned} \tag{26}$$

For a RG transformation, we subdivide the modes in Fourier space into two parts: One set with $\Lambda/b < |\mathbf{q}| \le \Lambda$ which we integrate over and obtain a trivial part $V\delta f_b$, and a second set with $0 \le |\mathbf{q}| \le \Lambda/b$ which we shall keep. The second step of the RG transformation is to recover the up limit of integration back to Λ by the rescaling $\mathbf{q}' = b\mathbf{q}$. In the third step of RG, we shall renormalize the fields according to $\phi_p'(\mathbf{q}') = \phi_p(\mathbf{q}')/z$, and $\phi_r'(\mathbf{q}') = \phi_r(\mathbf{q}')/y$. The resulting recursion relations are thus

$$\begin{cases} t' = z^2 b^{-d} t \\ K' = z^2 b^{-d-2} K \\ L' = z^2 b^{-d-4} L \\ s' = y^2 b^{-d} s \\ m' = zy b^{-d} m \\ u' = z^4 b^{-3d} u \\ v' = y^4 b^{-3d} v \\ w' = z^2 y^2 b^{-3d} w. \end{cases} \tag{27}$$

One fixed point is to set $K' = K$, $s' = s$, which indicates:

$$z = b^{1+d/2}, \quad y = b^{d/2}, \tag{28}$$

$$\Rightarrow \quad \begin{cases} y_t = 2,\ y_L = -2,\ y_m = 1, \\ y_u = 4-d,\ y_v = -d,\ y_w = 2-d. \end{cases} \tag{29}$$

This result means that when the the fluctuations scale for protein and the "mass" scale for RNA are invariant, there are three relevant operators: t, m, and u (when $d = 3$). Therefore, when L, v and w close to zero, the singular part of the free energy is

$$\begin{aligned} f_{\text{sing}} &= b^{-d} f(b^{y_t}t, b^{y_m}m, b^{y_u}u) \\ &= b^{d/y_t} f\big(1, \frac{m}{t^{y_m/y_t}}, \frac{u}{t^{y_u/y_t}}\big) \\ &= t^{2-\alpha} g\big(\frac{m}{t^{\Delta_m}}, \frac{u}{t^{\Delta_u}}\big). \end{aligned} \tag{30}$$

$$\therefore \quad \begin{cases} \nu = 1/y_t = \frac{1}{2} \\ \alpha = 2 - d\nu = \frac{1}{2} \\ \Delta_m = y_m/y_t = \frac{1}{2} \\ \Delta_u = y_u/y_t = \frac{1}{2}. \end{cases} \tag{31}$$

There could be another fixed point by setting $t' = t$ and $s' = s$, where we have:

$$z = b^{d/2}, \quad y = b^{d/2}, \tag{32}$$

$$\Rightarrow \quad \begin{cases} y_K = -2,\ y_L = -4,\ y_m = 0, \\ y_u = -d,\ y_v = -d,\ y_w = -d. \end{cases} \tag{33}$$

Though, this is not a typical fixed point, since there is only one marginal operator m. As we can see, the mutual interaction between protein and RNA molecules to the lowest-order m is always non-degenerate, which means such a mutual interaction is an important player in determining the phase-transition behavior in the vicinity of the critical point when multiple participants are involved. Biologically speaking, RNA is potentially interacting with protein condensates and influence the phase-separation behavior.

The Perturbative RG of Gaussian model

A more formal way to perform RG is to do perturbative correction based on Gaussian kernel. Since there are two fields in this case, I'm not 100% sure about my attempt of generalizing the Gaussian perturbative RG to two fields. I put this framework in the Supplement and will further validate.

DYNAMIC FEEDBACK FROM NASCENT RNA TRANSCRIPTION

Transcriptional proteins (TPs) are far more than interactive particles in a tube. If they are adjacent to an active transcription site, TPs will start to produce RNAs *in situ*, which, in turn, will have instant feedback to the phase separation behavior of nearby TPs. Therefore, in this section, I will go beyond the thermodynamic-governed equilibrium, and explore the non-equilibrium dynamics of RNA-protein interaction coupled to *in situ* transcription.

Transcription feedback prompts the nucleation

In the context of equilibrium, we have studied the size dependence of pre-existing transcriptional condensates upon RNA-protein charge interaction, and have explained the nucleation process as a first-order phase transition resulting from supersaturation. However, such a nucleation mechanism may not be true, because in a real cell the chemical potentials of proteins are far below the case of supersaturation, otherwise everything aggregates easily and cell will die. Some regulated, active process has to happen in order to recruit appropriate TPs to the required locations. Such a process could be *in situ* transcription.

To get correct intuition, I started from real experiments to test the rule of transcription feedback upon nucleation. I treated cells either with DRB (a removable transcription inhibitor) or FVP (stands for flavopiridol, which is an irreversible transcription inhibitor) to stop the transcription, and then added hexanediol (an organic compound that interrupts all IDR interactions) to dissolve pre-existing Mediator condensates. After that, I tired to remove the inhibitor from the dish by washing with fresh media. If transcription is really crucial for nucleation, then I should be able to observe the reappearance of mediator condensates if the transcription inhibitor is truly removed. The experimental results are in FIG. 6, which is consistent with my prediction–after washing away DRB, transcription is recovered thus mediator condensates are re-nucleated; after washing away FVP, transcription is still permanently disabled (because FVP is an irreversible transcription inhibitor) thus mediator condensates couldn't recover.

Based on experimental evidence, we can extend Eq. 1 to the non-equilibrium realm by applying it to a set of reaction-diffusion equations:

$$\begin{aligned}\partial_t\phi_p(\mathbf{x},t) &= D_p\nabla^2\Big(\frac{\partial\,\beta\Psi}{\partial\phi_p}\Big),\\ \partial_t\phi_r(\mathbf{x},t) &= D_r\nabla^2\Big(\frac{\partial\,\beta\Psi}{\partial\phi_r}\Big)+\delta(\mathbf{x})k_p\phi_p-k_d\phi_r,\end{aligned}\quad(34)$$

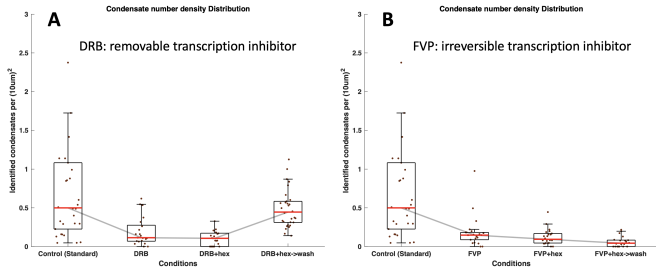

FIG. 6: Experimental test of the active transcription induced nucleation of Mediator condensates. DRB stands for 5,6-Dichlorobenzimidazole 1-β-D-ribofuranoside; hex stands for 1,6-Hexanediol.

where $D_{p,r}$ are diffusion coefficients. An active transcription site is placed at the origin with transcription rate k_p. RNAs are assumed to degrade with the rate k_d, while TPs are assumed to be stable. More details about derivation and implementation of Eq. 34 can be found in Supplements.

A simulation in 3-d lattice is shown in FIG. 7. As we can see, when starting with an initial enrichment of TPs at origin, a *in situ* transcription-seeded nucleation can happen. To validate that sufficient transcription feedback is a requisite for the nucleation to happen, I reduced the transcription rate k_p by different folds, starting from the original setup $k_p = k_p^0$. The *in situ* concentration of TPs are shown in FIG. 8. Clearly, when the transcription rate is not strong enough, the initial recruited TPs will diffuse away before being stabilized by nascent RNAs. Consequently, we conclude that nascent transcription feedbacks and seeds the nucleation of transcriptional proteins *in situ*.

In situ degradation of long RNA stabilize the nucleation

Some of my experimental results indicate that insufficient degradation/trimming of overlong RNAs (e.g., in the *Exosc3* knock-out cell line) undermines the nucleation of transcriptional condensates (data not shown). To test this observation, I firstly start with setting a high charge (i.e. long length) $\rho = 7.5\rho_0$, and I found that the transcriptional condensate cannot grow properly (FIG. 9A). It is not hard to be foreseen: very long RNAs are physically excluding the occupation of transcriptional proteins, thus volumetric-saturation effect becomes significant before charge-balance is achieved.

Recent researches also indicate that RNA Exosome is performing RNA trimming/degradation *in situ* [11, 12], thus it is reasonable to incorporate the degradation feature of RNA Exosome as a converting rate k_s at the transcriptional site together with an additional RNA field

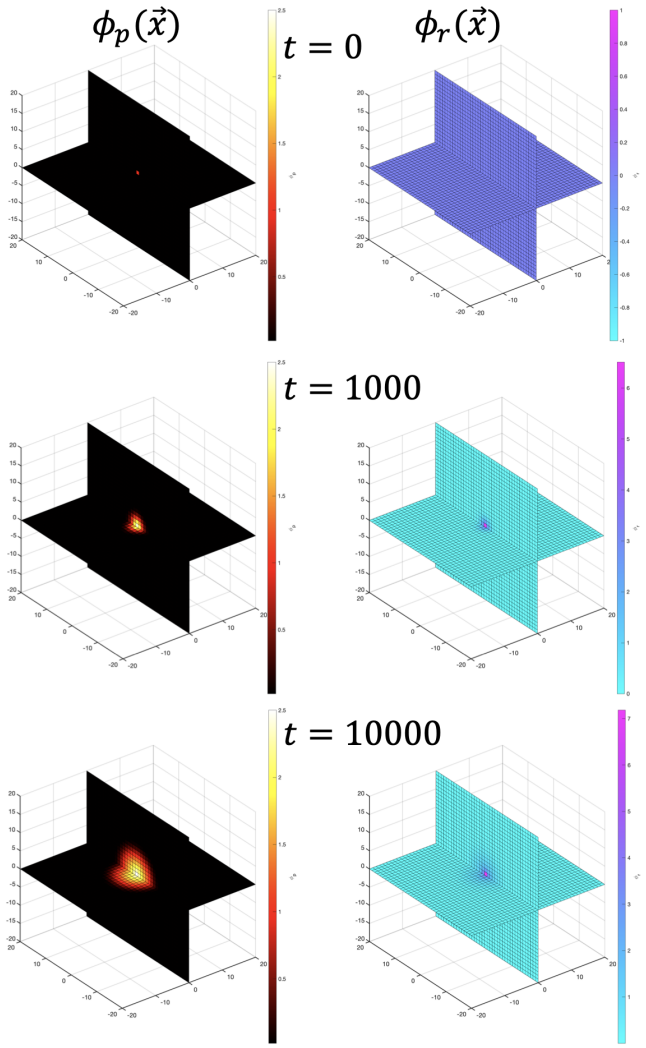

FIG. 7: Simulation of reaction-diffusion of protein-RNA. Lattice-spacing and diffusion coefficient of protein is set to 1. 2-d slices at iteration step of 0, 1000, and 10000 are shown.

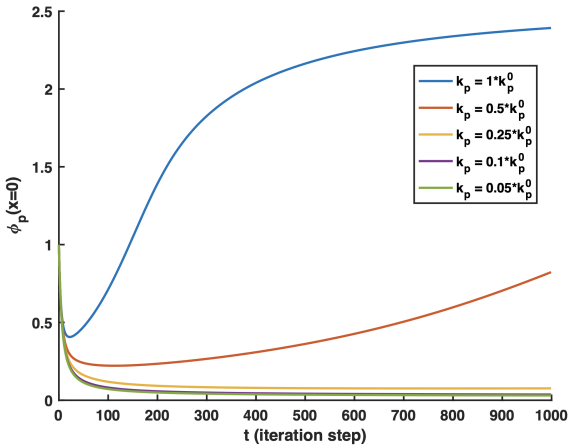

FIG. 8: Sufficient transcriptional feedback is required for transcriptional proteins to conquer the nucleation barrier.

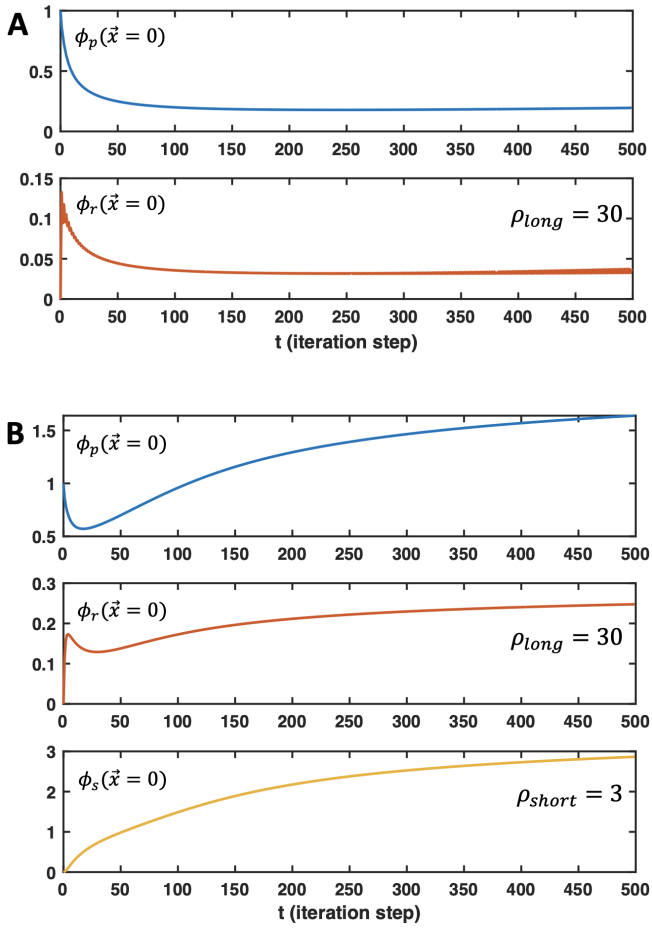

FIG. 9: The *in situ* degradation of long RNA stabilize the nucleation. (A) The model with a single long RNA population has the trouble of nucleation. (B) The model with an additional converting rate to a second shorter RNA population can secure the nucleation.

$\phi_s(\mathbf{x}, t)$ of shorten length:

$$\begin{aligned}
\frac{\partial \phi_p(\mathbf{x},t)}{\partial t} &= \nabla^2\Big(\frac{\partial \Psi_2}{\partial \phi_p}\Big), \\
\frac{\partial \phi_r(\mathbf{x},t)}{\partial t} &= \nabla^2\Big(\frac{\partial \Psi_2}{\partial \phi_r}\Big) + \delta(\mathbf{x})(k_p\phi_p - k_s\phi_r) - k_d\phi_r, \\
\frac{\partial \phi_s(\mathbf{x},t)}{\partial t} &= \nabla^2\Big(\frac{\partial \Psi_2}{\partial \phi_s}\Big) + \delta(\mathbf{x})k_s\frac{\phi_r}{\rho_s} - k_d\phi_s. \qquad (35)
\end{aligned}$$

More details about formulating Ψ_2 from Eq. 1 can be found in Supplements (Eq. 56). By implementing this dual-RNA population model with an initially highly charged long RNA, the nucleation process is able to be re-secured (FIG. 9B). This result successfully recapitulated why TPs have the trouble to re-nucleate in the *Exosc3* knock-out cell line but not in the intact cell line.

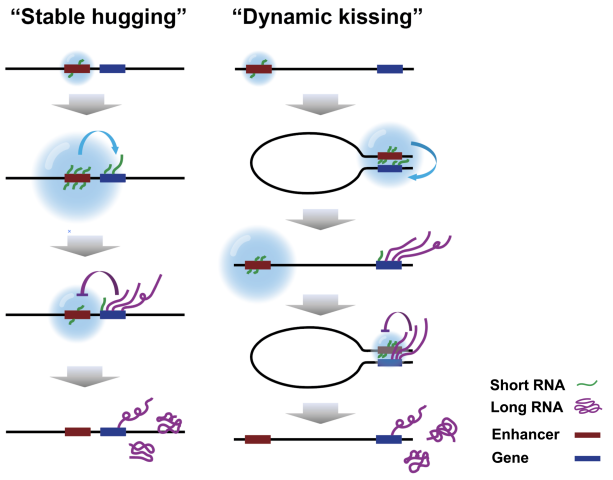

FIG. 10: Conceptional manners of dynamical interactions between enhancer and promoter (gene) via phase-separated transcriptional condensates.

Implement genome structure into the phase-separation underlain protein-RNA interactions

Once a transcriptional condensate is nucleated and stabilized at enhancer, it can dynamically contact with the nearby promoter region via chromatin looping thus trigger the transcription burst, whereupon the nascent mRNAs will feedback to the adjacent condensate who triggered the burst. The exact feed-forward and feedback manner could be decided by the geometric size of a transcriptional condensate and the genomic structure between enhancer and promoter (FIG. 10). The theoretical framework and formulation of the dynamic enhancer-promoter interactions are attached in the Supplements.

DISCUSSION

In this work, I used field approach to study the phase-separation behaviors of transcriptional condensates relating to RNA-protein interactions. In the equilibrium limit, via grand ensemble formulation, I found the increased length of RNA will "buffer" the transcriptional proteins thus undermine the condensate size; By performing saddle point approximation at critical point, I found the relative strength between self and mutual interactions will decide whether the system undergoes a phase-transition into a mixed or a demixed phase; Renormalization group analysis unveils that the mutual interaction is always a non-irrelevant component, which indicates the importance of RNA-protein interaction in determining the critical phase-transition behavior. In the non-equilibrium limit, by performing reaction-diffusion equations, I found nascent transcription could be crucial to properly seed the nucleation of transcriptional condensate. *In situ* degradation/trimming of overlong RNA into small pieces will secure the nucleation. Most theoretical and simulation findings are either directly confirmed with my recent experiments or are inferred from previously published works.

In the future, I will complete the following up work regarding the perturbative RG of Gaussian model as well as the dynamical interactions between enhancer and promoter (gene).

[1] Shin, Y., & Brangwynne, C. P., *Science*: 357,6357. (2017).
[2] Cho, W. K., Spille, J. H., et al., *Science*: 361(6400), 412-415. (2018).
[3] Boija, A., Klein, I. A., et al., *Cell*: 175(7), 1842-1855. (2018).
[4] Sabari, B. R., Dall'Agnese, et al., *Science*: 361(6400). (2018).
[5] Cisse, I. I., at al., *Science*: 341(6146), 664-667. (2013).
[6] Alexander, J. M., *elife*: 8, e41769. (2019).
[7] Henninger, J. E., Oksuz, O., Shrinivas, K., et al., *Cell*: 184(1), 207-225. (2021).
[8] Maharana S., et al., *Science*: 360, 918–921. (2018).
[9] Narayanan, A., et al., *eLife*: 8:e39695. (2019).
[10] Ogami K., et al., *MDPI*. (2018).
[11] Pefanis E., et al., *Cell*: 161, 774–789. (2015).
[12] Lim J., et al., *Cell*: 169, 523–537. (2017).

SUPPLEMENTS

Model Reparameterization

Let's start by writing down the full potential energy density $\tilde{\Psi}_V$ at each point $\mathbf{x}$ involving the volumetric fields of protein $\varphi_p(\mathbf{x})$ and RNA $\varphi_r(\mathbf{x})$:

$$\begin{aligned}\beta\tilde{\Psi}_V\left[\varphi_p(\mathbf{x}),\varphi_r(\mathbf{x})\right] &= \frac{A}{2}[\varphi_p^2 - a]\cdot[(\varphi_p-\varphi_p^c)^2 - b] \\ &+ \frac{K}{2}|\nabla\varphi_p|^2 + \frac{L}{2}|\nabla^2\varphi_p|^2 + \frac{B}{2}(\frac{\varphi_r}{\upsilon})^2 + M\varphi_p\frac{\varphi_r}{\upsilon} \\ &+ \frac{E}{2}(\varphi_p - \frac{\rho\varphi_r}{\upsilon})^2 + S\varphi_r^4 + W\varphi_p^2\varphi_r^2, \end{aligned} \tag{36}$$

where $\beta = (k_BT)^{-1}$. In this model, A and B represent the self-interaction of protein and RNA to the lowest order, respectively. The depth of the dual-well potential of protein in dilute and condensed phases are tunable by a and b, respectively. For simplicity, $a \equiv 0$ in this note. K and L capture the surface tension of protein droplets to the lowest order. M stands for the mutual interaction between RNA and protein to the lowest order (the law of mass action). E is the coefficient describing the electrostatic balance of RNA and protein to the lowest order. S and W are additional 4^{th}-order penalty factors that constrain the saturation volume of RNA and protein within

each voxel. φ_p^c is the optimized volume fraction of proteins in the condensed phase; υ is the molecular volume of RNA (the molecule volume of protein is defined as 1); ρ is the relative charge of each RNA to protein molecule, and should be proportional to the RNA length. Since only electromagnetic forces are considered in the energy density and such interactions (e.g. electric potential energy, spin-spin coupling, dipole-dipole interaction, and etc.) are invariant a charge conjugation in the realm of classical field theory, thus only even-order terms survive in this model.

If we rescale φ_p by φ_p^c and φ_r by $S^{-\frac{1}{4}}\upsilon$, and redefine all parameters by carefully tracking the dimensionality, we can obtain the dimensionless fields of protein $\phi_p(\mathbf{x})$ and RNA $\phi_r(\mathbf{x})$:

$$\begin{aligned}\beta\Psi\left[\phi_p(\mathbf{x}),\phi_r(\mathbf{x})\right] &= \frac{A}{2}\phi_p^2[(\phi_p-1)^2-b]\\ &+ \frac{K}{2}|\nabla\phi_p|^2+\frac{L}{2}|\nabla^2\phi_p|^2+\frac{B}{2}\phi_r^2-M\phi_p\phi_r\\ &+ \frac{E}{2}(\phi_p-\rho\phi_r)^2+S\phi_r^4+W\phi_p^2\phi_r^2. \end{aligned} \tag{37}$$

Let's be aware of some facts of these parameters. M is proportional to ρ, and is forced to be positive since this factor mainly accounts for the direct attraction between RNA and RNA binding sites of proteins. $S\equiv\upsilon^4$ and $W\propto\upsilon^2$ after redefinition. Therefore, υ is effectively tuning the maximum capacity of RNA per voxel in this model. Notice that RNA is a fluctuating polymer, whose radius is proportional with $\sqrt{\rho}$ (given that $\langle R^2\rangle\propto\rho\xi_p$ to ξ_p being the persistence length); therefore, $\upsilon\propto\rho^{1.5}$. Given a specific ξ_p for RNA, the volumetric penalty factors yield $S\propto\rho^6$ and $W\propto\rho^3$.

When $\phi_p,\phi_r\mapsto 0$ and uniformly distributed, the system should recover to the free-diffusion scenario under non-interacting condition (i.e. $M=0$ and $E=0$), which yields:

$$\mathbf{J}=-D\nabla\phi, \tag{38}$$

where D is the diffusion coefficient and $\mathbf{J}$ is the resulting diffusion flux. On the other hand, the Fick's first law of a chemical system other than ideal solutions or mixtures requires that:

$$\mathbf{J}=-\frac{D}{k_BT}\nabla\Big(\frac{\partial\Psi}{\partial\phi}\Big). \tag{39}$$

The compatiblity of these two equations yields:

$$\frac{\partial(\beta\Psi)}{\partial\phi_p}\Big|^{(M,E=0)}_{\phi_p\mapsto 0,\phi_r=0} = \phi_p+\mathcal{O}(\phi_p)^2, \tag{40}$$

$$\frac{\partial(\beta\Psi)}{\partial\phi_r}\Big|^{(M,E=0)}_{\phi_r\mapsto 0,\phi_p=0} = \phi_r+\mathcal{O}(\phi_r)^2. \tag{41}$$

These two equations claim the following constrains to the parameters:

$$A\cdot(1-b)=1,\quad B=1. \tag{42}$$

ΔE_{hoop}	$0.032k_BT$	k_BT	$2k_BT$	$3k_BT$
A	1	2.385	3.618	4.825
b	0	0.581	0.724	0.793

TABLE I: Typical energy barriers and corresponding parameter value.

In the dual-well potential of the proteins, the energy difference from the summit between dilute/condense phases to the bottom of the condense phase determines how stable a protein condensate is solely by protein multivalency interactions (which is the energy barrier for a protein molecule to hoop from the condensed phase to the the dilute phase, ΔE_{hoop}). Several typical values are numerically solve as in Table. I. Given that a typical stable condensate holds at least hundreds of molecules (refer to [2]) to survive from thermo-fluctuation ($E_{\text{condense}}\geq 3k_BT$), thus the energy barrier per molecule due to enhanced IDR interaction in condensed phase (i.e. ΔE_{hoop}) is roughly $3k_BT/100=0.03k_BT$, which is exactly the case when $A=1$. Therefore, unless there is a specific clarification, we shall set $A=1$, $B=0$ in context.

Therefore, the **final energy density** that we are going to study with the lowest reasonable orders and fewest number of free parameters is:

$$\begin{aligned}\beta\Psi\left[\phi_p(\mathbf{x}),\phi_r(\mathbf{x})\right] &= \frac{A}{2}\phi_p^2[\phi_p^2-2\phi_p+\frac{1}{A}]\\ &+ \frac{K}{2}|\nabla\phi_p|^2+\frac{L}{2}|\nabla^2\phi_p|^2+\frac{1}{2}\phi_r^2-M\phi_p\phi_r\\ &+ \frac{E}{2}(\phi_p-\rho\phi_r)^2+S\phi_r^4+W\phi_p^2\phi_r^2. \end{aligned} \tag{43}$$

Diffusion-Reaction around a Transcription Site

We start with writing the general RNA-protein dynamical model:

$$\begin{aligned}\partial_t\phi_p(\mathbf{x},t) &= -\nabla\cdot\mathbf{J}_p,\\ \partial_t\phi_r(\mathbf{x},t) &= -\nabla\cdot\mathbf{J}_r+\delta(\mathbf{x})k_p\phi_p-k_d\phi_r. \end{aligned} \tag{44}$$

We assume the degradation rate of protein is negligible compared with RNA, and transcriptional proteins are actively producing RNA at the transcription site placed at the origin. The dimension of a tiny transcription is roughly the scale of the DNA persistence length ($\sim 50\,nm$), while the dimension of a typical phase-separated transcriptional condensate is $\sim 500\,nm$. Therefore, is reasonable to regard the transcription site as a delta function of the voxel size. The diffusion coefficients of large protein complexes and RNAs are roughly comparable ($\sim 1\,\mu m^2/s$), thus we shall rescale the time such that $D=1$ for both RNA and protein for the simplicity of derivation. However, the relative diffusion of RNA and

protein is still allowed to be tuned in simulations. Appropriately evaluating the local chemical potential and accordingly the molecule flux is critical for the dynamical model to be meaningful. Here I provide two approaches.

Chemical potential evaluation I: Variational derivative of local voxel

Here, the chemical potential of each block (voxel) is estimated by changing the molecule density inside the voxel while keeping other blocks fixed. This method is only valid under huge number assumption, since the "perturbation" here actually breaks conservation of total number of molecules inside the system. Accordingly, the diffusion flux of protein can be locally differentially evaluated as:

$$\begin{aligned}\mathbf{J}_p &= -\nabla\Big(\frac{\partial(\beta\Psi)}{\partial\phi_p}\Big) = \nabla[(M+\rho E)\phi_r \\ &\quad -(1+E+2W\phi_r^2)\phi_p + 3A\phi_p^2 - 2A\phi_p^3] \\ &\quad -\nabla(\text{“gradient terms”}),\end{aligned} \tag{45}$$

where ∇ of two gradient terms are expressed as (note ϕ_p as ϕ for simplicity):

$$\begin{aligned}&\nabla_j(\text{“1}^{\text{st}}\text{-order gradient term”}) \\ =\ & \frac{\partial}{\partial x_j}\Big\{\frac{\partial}{\partial(\partial_k\phi)}\Big[\frac{K}{2}\partial^i\phi\partial_i\phi\Big]\cdot\frac{\delta(\partial^k\phi)}{\delta\phi}\Big\} \\ =\ & K\frac{\partial}{\partial x_j}\Big\{\partial_k\phi\cdot\frac{\delta(\partial^k\phi)}{\delta\phi}\Big\} \\ =\ & K\partial_j\partial_k\phi\cdot\frac{\delta(\partial^k\phi)}{\delta\phi} + K\partial_k\phi\cdot\frac{\delta(\partial_j\partial^k\phi)}{\delta\phi},\end{aligned} \tag{46}$$

and

$$\begin{aligned}&\nabla_j(\text{“2}^{\text{nd}}\text{-order gradient term”}) \\ =\ & \frac{\partial}{\partial x_j}\Big\{\frac{\partial}{\partial(\partial_k\partial_l\phi)}\Big[\frac{L}{2}(\partial^i\partial_i\phi)^2\Big] : \frac{\delta(\partial^k\partial^l\phi)}{\delta\phi}\Big\} \\ =\ & L\frac{\partial}{\partial x_j}\Big\{\partial_k^2\phi\cdot\frac{\delta(\partial_k^2\phi)}{\delta\phi}\Big\} \\ =\ & L\partial_j\partial_k^2\phi\cdot\frac{\delta(\partial_k^2\phi)}{\delta\phi} + L\partial_k^2\phi\cdot\frac{\delta(\partial_j\partial_k^2\phi)}{\delta\phi}.\end{aligned} \tag{47}$$

In these two expressions, Einstein notation is applied and $\frac{\delta\varphi}{\delta\phi}$ is the functional derivative of $\varphi(\mathbf{x})$ with respect to $\phi(\mathbf{x})$. Although different orders of derivative should be regarded as independent functions in principle, the secondary derivatives for each direction is numerically related to its original function at the same position. For instance:

$$\begin{aligned}&\because\quad f_{xx}(x,y) \approx \frac{f(x+a,y)+f(x-a,y)-2f(x,y)}{a^2}, \\ &\therefore\quad \frac{\delta f_{xx}}{\delta f}\Big|_{(x,y)} \approx -\frac{2}{a^2}.\end{aligned} \tag{48}$$

Therefore, after coarse-graining the space, we have

$$\nabla(\text{“gradient terms”}) \approx -\frac{2}{a^2}\nabla(K\phi + L\nabla^2\phi), \tag{49}$$

where a is the lattice unit size. The RNA flux $\mathbf{J}_r$ can mimic the expression of Eq. 45 without taking care of the gradient terms. Consequently, the **final reaction-diffusion model** is formulated as:

$$\begin{aligned}\partial_t\phi_p(\mathbf{x},t) &= \nabla^2[-(M+\rho E)\phi_r + 2W\phi_p\phi_r^2 - \frac{2L}{a^2}\nabla^2\phi_p \\ &\quad +(1+E-\frac{2K}{a^2})\phi_p - 3A\phi_p^2 + 2A\phi_p^3],\end{aligned} \tag{50}$$

$$\begin{aligned}\partial_t\phi_r(\mathbf{x},t) &= \nabla^2[-(M+\rho E)\phi_p + (1+\rho^2E)\phi_r + 4S\phi_r^3 \\ &\quad +2W\phi_p^2\phi_r] + \delta(\mathbf{x})k_p\phi_p - k_d\phi_r.\end{aligned} \tag{51}$$

As we can see, the "1$^{\text{st}}$-order gradient term$''$ effectively reduce the self-energy parameter of protein in each voxel by a factor of $2K/a^2$.

Chemical potential evaluation II: Minimization of action integral

In this method, the action is defined as the global Hamiltonian:

$$\begin{aligned}&\beta\mathcal{H}\big[\phi_p(\mathbf{x}),\phi_r(\mathbf{x})\big] = \int_V d^d\mathbf{x}\Big\{\frac{A}{2}\phi_p^2[\phi_p^2 - 2\phi_p + \frac{1}{A}] \\ &+\ \frac{K}{2}|\nabla\phi_p|^2 + \frac{L}{2}|\nabla^2\phi_p|^2 + \frac{1}{2}\phi_r^2 - M\phi_p\phi_r \\ &+\ \frac{E}{2}(\phi_p-\rho\phi_r)^2 + S\phi_r^4 + W\phi_p^2\phi_r^2\Big\}.\end{aligned} \tag{52}$$

Now, if $\phi_p(\mathbf{x})$ and $\phi_r(\mathbf{x})$ are varied by a small function $\epsilon g_p(\mathbf{x})$ and $\epsilon g_r(\mathbf{x})$, respectively, then to the order of ϵ, the Hamiltonian change the amount of

$$\begin{aligned}&\beta\mathcal{H}\big[\phi_p(\mathbf{x})+\epsilon g_p,\phi_r(\mathbf{x})+\epsilon g_r\big] - \beta\mathcal{H}\big[\phi_p(\mathbf{x}),\phi_r(\mathbf{x})\big] \\ &= \int_V d^d\mathbf{x}\Big\{\big[-(M+\rho E)\phi_r + 2W\phi_p\phi_r^2 + (1+E)\phi_p \\ &-3A\phi_p^2 + 2A\phi_p^3 - K\nabla^2\phi_p + L\nabla^2(\nabla^2\phi_p)\big]\cdot\epsilon g_p \\ &+\big[-(M+\rho E)\phi_p + (1+\rho^2E)\phi_r + 4S\phi_r^3 \\ &+2W\phi_p^2\phi_r\big]\cdot\epsilon g_r\Big\} + \mathcal{O}(\epsilon^2).\end{aligned} \tag{53}$$

Here, we have used Gauss's theorem, such that

$$\begin{aligned}\int_V d^d\mathbf{x}\,\nabla g\cdot\nabla f &= \int_V d^d\mathbf{x}\,\nabla\cdot(g\nabla f) - \int_V d^d\mathbf{x}\,g\nabla^2 f \\ &= \oint_S d\mathbf{s}\cdot g\nabla f - \int_V d^d\mathbf{x}\,g\nabla^2 f \\ &= -\int_V d^d\mathbf{x}\,g\nabla^2 f,\end{aligned} \tag{54}$$

Where f is any arbitrary well-defined scalar field and g is a perturbation function with boundary condition $g(\mathbf{x} \in S) = 0$.

Therefore, in Eq. 53, the part multiplied by "ϵg_p" is the chemical potential of protein. Accordingly, Eq. 50 should be modified to:

$$\partial_t \phi_p(\mathbf{x},t) = \nabla^2\big[-(M+\rho E)\phi_r + (1+E+2W\phi_r^2)\phi_p - 3A\phi_p^2 + 2A\phi_p^3 - K\nabla^2\phi_p + L\nabla^2(\nabla^2\phi_p)\big]. \quad (55)$$

One should be aware that this evaluation is valid only when the whole system is under quasi-static process in order for the stationary action principle to be reasonable, which indicates $k_p, k_d \ll 1$ (as we already assumed the diffusion coefficient $D = 1$).

Two RNA populations

A more detailed modification is to allow Exosome to degrade RNA to smaller pieces *on foci*, then we should have another field function $\phi_s(\mathbf{x},t)$ to represent another shorten-RNA population. The corresponding energy density should be modified as:

$$\begin{aligned}\beta\Psi_2\left[\phi_p(\mathbf{x}),\phi_r(\mathbf{x}),\phi_s(\mathbf{x})\right] &= \frac{A}{2}\phi_p^2[\phi_p^2 - 2\phi_p + \frac{1}{A}] \\ &+ \frac{K}{2}|\nabla\phi_p|^2 + \frac{L}{2}|\nabla^2\phi_p|^2 + \frac{1}{2}\phi_r^2 + \frac{1}{2}\phi_s^2 \\ &- M\phi_p(\phi_r + \rho_s\phi_s) + \frac{E}{2}[\phi_p - \rho\phi_r - \rho\rho_s\phi_s]^2 \\ &+ S[\phi_r^4 + (\upsilon_s\phi_s)^4] + W\phi_p^2\cdot[\phi_r^2 + (\upsilon_s\phi_s)^2]. \end{aligned} \quad (56)$$

ρ_s and υ_s are the relative charge (or say, length) and volume of shorten RNAs compared with these of the intact RNAs, respectively; typically, $\rho_s < 1$. If we model both RNAs as random-walking polymers, then $\upsilon_s = \rho_s^{\frac{3}{2}}$. The reaction-diffusion model should also be changed accordingly:

$$\begin{aligned}\frac{\partial\phi_p(\mathbf{x},t)}{\partial t} &= \nabla^2\Big(\frac{\partial\Psi_2}{\partial\phi_p}\Big), \\ \frac{\partial\phi_r(\mathbf{x},t)}{\partial t} &= \nabla^2\Big(\frac{\partial\Psi_2}{\partial\phi_r}\Big) + \delta(\mathbf{x})(k_p\phi_p - k_s\phi_r) - k_d\phi_r, \\ \frac{\partial\phi_s(\mathbf{x},t)}{\partial t} &= \nabla^2\Big(\frac{\partial\Psi_2}{\partial\phi_s}\Big) + \delta(\mathbf{x})k_s\frac{\phi_r}{\rho_s} - k_d\phi_s. \end{aligned} \quad (57)$$

Alternatively, a simplified way to introduce preferential degradation *on foci* is to incorporate an additional part degradation rate at the *on foci* position; in other words, the RNA degradation term $-k_d\phi_r$ is replaced as

$$-(k_d + \delta(\mathbf{x})k_d^{\Delta})\,\phi_r. \quad (58)$$

Grand Canonical Ensemble Construction

If we assume the densities of protein and RNA inside a condensate are roughly uniform, we can write down the total energy of a condensate incorporating n_p number of protein molecules and n_r number of RNA molecules as

$$E_C(n_p,n_r) = a(n_p + \upsilon n_r)^{2/3} - bn_p + c(n_p - \rho n_r)^2. \quad (59)$$

In this expression, a is the surface-tension energy coefficient, b is the unit bulk energy gain due to protein-protein multivalency interactions, and c is the parameter constraining the overall protein-RNA charge balance. υ and ρ are again the relative volume and charge of a RNA molecule to those of a protein molecules, respectively. Notice that "$n_p + \upsilon n_r$" is proportional to the total volume, thus $(n_p + \upsilon n_r)^{2/3}$ scales with the surface area of the sphere.

When multiple nucleation sites present in a closed system, the partition function of N_p protein molecules and N_r RNA molecules can be written as:

$$Z(N_p,N_r) = \sum_{\{n_p,n_r\}} p(n_p^0,n_r^0)\times e^{-\beta\sum_s' E_C(n_p^s,n_r^s)}. \quad (60)$$

$p(n_p^0,n_r^0)$ represents the likelihood of having n_p^0 protein molecules and n_r^0 RNA molecules in the dilute phase. The comma $'$ on the summation indicates the total number of protein and RNA molecules from different condensates "s" are constrained by $(N_p - n_p^0)$ and $(N_r - n_r^0)$, respectively. If we assume that most molecules are in the dilute phase, then p is only significant when $n_p^0 \sim N_p$ and $n_r^0 \sim N_r$:

$$\begin{aligned} p(n_p,n_r) \;\propto\; e^{\log\Omega(n_p,n_r)} &\simeq \exp\Big\{\log\Omega(N_p,N_r) \\ &- \frac{1}{2}\frac{\partial^2\log\Omega}{\partial n_p^2}\Big|_{(N_p,N_r)}\cdot(N_p-n_p)^2 \\ &- \frac{1}{2}\frac{\partial^2\log\Omega}{\partial n_r^2}\Big|_{(N_p,N_r)}\cdot(N_r-n_r)^2\Big\} \end{aligned} \quad (61)$$

$$\begin{aligned} \because\quad \Omega(n_p,n_r) &= \frac{V^{n_p}\cdot V^{n_r}}{n_p!\cdot n_r!\cdot h^{n_p}\cdot(\upsilon h)^{n_r}}, \\ \therefore\quad \frac{\partial\log\Omega}{\partial n_p} &= \log\Big(\frac{V}{h}\Big) - \log n_p, \\ \frac{\partial\log\Omega}{\partial n_r} &= \log\Big(\frac{V}{\upsilon h}\Big) - \log n_r, \\ \therefore\quad \frac{\partial^2\log\Omega}{\partial n_{p,r}^2} &= \frac{1}{n_{p,r}}. \end{aligned} \quad (62)$$

Here the likelihood p is proportional to the is expanded around the expected total number of molecules N_p and N_r to the second order. V is the total volume and h is the uncertainty block of each protein. Two factorials are added thus the entropy is extensive. Stirling's formula is applied when taking the logarithm of factorial.

$$Z(N_p,N_r) = \sum_{\{n_p,n_r\}} e^{-\frac{(N_p-n_p^0)^2}{2N_p} - \frac{(N_p-r_r^0)^2}{2N_r}}\times e^{-\beta\sum_s' E_C(n_p^s,n_r^s)}. \quad (63)$$

To make this model mathematically friendly, we can release the rigid constrain of total number of molecules available; instead, we introduce the fugacities w and z for each protein and RNA molecule to be partitioned from the dilute phase into a condensate, respectively. The consequent grand canonical partition function is:

$$\Xi(w,z) = \sum_{\substack{N_p=1\\N_r=0}}^{\infty} w^{N_p} z^{N_r} \sum_{\{n_p,n_r\}'} e^{-\beta \sum_s' E_C(n_p^s, n_r^s)}. \quad (64)$$

Under this configuration, the dilute phase is automatically eliminated (The comma $'$ on brace beneath the summation indicates there is no dilute phase in the set). The validity of such a conversion from Eq. 63 to Eq. 64 is guaranteed by the fact that a binomial distribution is approximating Gaussian in large number limit. Since N_p and N_r can now take any value, we can sum over the $\{n_p, n_r\}$ independently without any constraint for all the Λ condensates:

$$\Xi(w,z) = \Big(\sum_{n_p,n_r} w^{n_p} z^{n_r} e^{-\beta E_C(n_p,n_r)} \Big)^{\Lambda}. \quad (65)$$

Accordingly, the thermodynamic free energy is:

$$\begin{aligned} \mathcal{F} &= -k_B T \log \Xi \\ &= -\frac{\Lambda}{\beta} \log \big[\sum_{n_p,n_r} w^{n_p} z^{n_r} e^{-\beta E_C(n_p,n_r)} \big]. \end{aligned} \quad (66)$$

The fugacities are implicitly related to the expectation of total number of molecules in condensed phase as

$$\langle N_p \rangle = w \frac{\partial}{\partial w} \log \Xi, \quad \langle N_r \rangle = z \frac{\partial}{\partial z} \log \Xi. \quad (67)$$

To secure a overall neutral charge, the total number of protein and RNA molecules are constrained by

$$\langle N_p \rangle = \rho \langle N_r \rangle. \quad (68)$$

The average number of molecules per condensate is simply:

$$\langle n_{p,r} \rangle = \frac{\langle N_{p,r} \rangle}{\Lambda}. \quad (69)$$

Furthermore, the square mean of $N_{p,r}$ are

$$\begin{aligned} \langle N^2 \rangle &= \frac{1}{\Xi} y \frac{\partial}{\partial y} \Big[y \frac{\partial}{\partial y} \Xi \Big] \\ &= y \frac{\partial}{\partial y} \log \Xi + y^2 \frac{\partial^2}{\partial y^2} \log \Xi + \Big(y \frac{\partial}{\partial y} \log \Xi \Big)^2, \end{aligned} \quad (70)$$

where $y \mapsto w$ for $\langle N_p^2 \rangle$ and $y \mapsto z$ for $\langle N_r^2 \rangle$. On the other hand:

$$\langle N^2 \rangle = \Lambda \langle n^2 \rangle + \Lambda(\Lambda - 1) \langle n \rangle^2. \quad (71)$$

Therefore, the fluctuation of molecule number per condensate can be evaluated by variance as

$$\begin{aligned} \langle (n - \langle n \rangle)^2 \rangle &= \langle n^2 \rangle - \langle n \rangle^2 = \frac{1}{\Lambda} [\langle N^2 \rangle - \langle N \rangle^2] \\ &= \frac{1}{\Lambda} \big[y \frac{\partial}{\partial y} \log \Xi + y^2 \frac{\partial^2}{\partial y^2} \log \Xi \big]. \end{aligned} \quad (72)$$

Enhancer-promoter Interaction

Chromatin dynamics

Let's start with modeling a piece of chromatin as the non-interacting, self-avoiding random walk of a polymer:

$$W_d(\mathbf{R}, l) = g_d^l \exp\Big[-\frac{d|\mathbf{R}|^2}{4l\xi_p} \Big] \frac{1}{(4\pi l \xi_p / d)^{d/2}}, \quad (73)$$

where W is the probability distribution function of a polymer of linear length l with end-to-end being separated by $\mathbf{R}$ in d-dimension. g_d is the volumetic factor in d-dimension after taking self-avoid into consideration, and ξ_p is the persistence length of such a polymer. This probability distribution is identical to the Boltzmann weight of a Hookian spring connecting the end points of the polymer:

$$p(\mathbf{R}) \propto e^{\frac{-V(\mathbf{R})}{k_B T}}, \text{ with } V(\mathbf{R}) = \frac{J}{2} |\mathbf{R}|^2, \; J = \frac{k_B T d}{2 l \xi_p}. \quad (74)$$

The equation of motion can be described by Langevin equation at small Reynold numbers limit:

$$\dot{\mathbf{R}} = -\mu \nabla V + \boldsymbol{\eta}(t), \quad (75)$$

where μ is mobility and $\boldsymbol{\eta}$ is random force. The random forces have the following property:

$$\langle \boldsymbol{\eta}(t) \rangle = 0, \quad \langle \eta_i(t) \eta_j(t') \rangle = 2 D_{\text{eff}} \delta_{ij} \delta(t - t'), \quad (76)$$

where D_{eff} is the effective "diffusion" coefficient that describes the stochastic fluctuation of the end-to-end distance due to the entropic fluctuation of the polymer.

Because of the appearance of CTCF and cohesin binding sites across the DNA, chromatin tends to form looping structures, resulting in different topologically associating domains (TADs). Therefore, the probability for a pair of enhancer and promoter with a linear genomic distance l being separated by $\mathbf{R}$ within a TAD of linear genomic length L in 3-d is:

$$W_{\text{loop}}(\mathbf{R}, l, L) = W_3(\mathbf{R}, l) \cdot W_3(\mathbf{R}, L - l). \quad (77)$$

For simplicity, let's focus on two special cases:

$$\textbf{case 1:} \quad \lim_{L \gg l} W_{\text{loop}}(\mathbf{R}, l, L) = W_3(\mathbf{R}, l); \quad (78)$$

$$\textbf{case 2:} \quad \lim_{L - l \to l} W_{\text{loop}}(\mathbf{R}, l, L) = W_3(\mathbf{R}, l)^2. \quad (79)$$

For **case 1**, the looping effect is negligible and the chromatin behaves like an open polymer with $\langle|\mathbf{R}|^2\rangle = 2l\xi_p$; For **case 2**, the looping effect is maximized and $\langle|\mathbf{R}|^2\rangle = l\xi_p$, whose probability distribution can still be regarded as an open polymer with mean-square displacement truncated by half. Therefore, no matter for which cases, the $W_{\rm loop}$ remains as a Hookian spring with Boltzmann weight, hence Eq. 75 is still valid for describing the temporal dynamics of two ends on a loop (actually one can check that beside these two cases, such a polymer↦spring mapping is generally true for any loops constructed via Eq. 77).

Besides the equivalent Langevin equation Eq. 75, the dynamic separation of two ends on a loop can also be simulated by Monte Carlo sampling of allowed configurations of a polymer chain on a 3-d lattice.

Transcription of mRNA at promotor

Given the nascent transcription of mRNAs starting from a promotor can range from one to tens of thousands of base-pairs (here "nascent" refers to mRNAs still attaching to the DNA via RNA Polymerase and elongating), a precise description of the overall nascent transcripts would be the following Master equation:

$$\frac{dp_n}{dt} = \sum_{m\neq n} R_{nm}p_m - \sum_{m\neq n} R_{mn}p_n - k_n p_n, \qquad (80)$$

where $p_n(t)$ is the probability finding a nascent mRNA of n-bp ($n = 1, 2, ..., N$) at time t, and R_{mn} is the transition rate of a mRNA from length n to length m. If $m > n$, R_{mn} represent transcription elongation; If $m < n$, R_{mn} represent splicing. k_n describe the pre-mature termination rate of mRNA of length n. To complete the boundary conditions, we can also define $p_0(t)$ as the promotor activity at t (may be explained as the abundance of RNA Polymerases at promoter) and R_{10} being the rate of RNA Polymerase starting elongation. $R_{N+1,N}$ is defined as the detach rate of mature mRNA from terminator and $k_N \equiv 0$ to avoid over counting of detach.

This Master-equation based model is too complicated and hard to comprehend its behavior. To simplify the computation and analysis, we assume that there are only two stages for the transcription of mRNAs: ϑ_p stands for the quantity of short mRNAs around the promoter that just start transcription; ϑ_t stands for the quantity of long mRNAs around the terminator that are almost done with transcription and are about to detach. We further introduce ϖ as the number of RNA Polymerases (RNAPs) loaded at promoter and standing by for transcription. These three variables yields the following ordinary differential equations:

$$\begin{aligned}
\frac{d\varpi}{dt} &= k_{\rm ini}\phi_p - k_{\rm esc}\varpi,\\
\frac{d\vartheta_p}{dt} &= k_{\rm esc}\varpi - k_{\rm elo}\vartheta_p,\\
\frac{d\vartheta_t}{dt} &= k_{\rm elo}\vartheta_p - k_{\rm ter}\vartheta_t. \qquad (81)
\end{aligned}$$

$k_{\rm ini}$ is the RNA Polymerase initiation rate; $k_{\rm esc}$ is the promoter-escape rate; $k_{\rm elo}$ is the elongation rate; $k_{\rm ter}$ is the transcription termination. In this model, the local transcriptional-protein density (noted by ϕ_p) are assumed to be proportional to the initiation activity of RNAPs on the promoter.

The whole model

Let's firstly introduce an additional mRNA field $\psi(\mathbf{x})$ to distinguish from the enhancer RNA field $\phi_r(\mathbf{x})$ as in Eq. 43. Therefore, the energy density should be modified to:

$$\begin{aligned}
&\beta\Psi_3\left[\phi_p(\mathbf{x}), \phi_r(\mathbf{x}), \psi(\mathbf{x})\right]\\
=\ & \frac{A}{2}\phi_p^2[\phi_p^2 - 2\phi_p + \frac{1}{A}] + \frac{K}{2}|\nabla\phi_p|^2 + \frac{L}{2}|\nabla^2\phi_p|^2\\
+\ & \frac{1}{2}\phi_r^2 + \frac{1}{2}\psi^2 - M\phi_p(\phi_r + \rho_m\psi)\\
+\ & \frac{E}{2}[\phi_p - \rho\phi_r - \rho\rho_m(\psi + \delta(|\mathbf{x}-\mathbf{R}|)\vartheta_t)]^2\\
+\ & S[\phi_r^4 + (\upsilon_m\psi)^4] + W\phi_p^2\cdot[\phi_r^2 + (\upsilon_m\psi)^2]. \qquad (82)
\end{aligned}$$

ρ_m and υ_m are the relative charge (or say, length) and volume of mRNA compared with eRNA, respectively; typically, $\rho_m > 1$. If we model both enhancer RNA and mRNA as random-walking polymers, then $\upsilon_m = \rho_m^{\frac{3}{2}}$. The on-foci mature mRNAs ϑ_t at location $\mathbf{R}$ contribute extra charge to the energy density. The diffusion-reaction equations are thus:

$$\begin{aligned}
\frac{\partial\phi_p(\mathbf{x},t)}{\partial t} &= \nabla^2\Big(\frac{\partial\Psi_3}{\partial\phi_p}\Big),\\
\frac{\partial\phi_r(\mathbf{x},t)}{\partial t} &= \nabla^2\Big(\frac{\partial\Psi_3}{\partial\phi_r}\Big) + \delta(\mathbf{x})k_p\phi_p - k_d\phi_r,\\
\frac{\partial\psi(\mathbf{x},t)}{\partial t} &= \nabla^2\Big(\frac{\partial\Psi_3}{\partial\psi}\Big) + \delta(|\mathbf{x}-\mathbf{R}|)k_{\rm ter}\vartheta_t - k_d\psi. \qquad (83)
\end{aligned}$$

Here, the enhancer has been forced to fix at the origin and promoter is at $\mathbf{R}$, where $\mathbf{R}(t)$ is determined via either Langevin equation in Eq. 75 or Monte Carlo sampling of polymer chain on 3-d lattice. The mRNA produce term $k_{\rm ter}\vartheta_t$ at location $\mathbf{R}$ is calculated from the third ODE in Eq. 81, and the RNAP loading rate described by the first ODE is always decided by the transcriptional-protein density ϕ_p at location $\mathbf{x} = \mathbf{R}(t)$.

The Perturbative RG of Gaussian model

Starting from Eq. 25, I going to propose a framework of perturbative RG of Gaussian model with two interacting fields. The first step is cross-grain, where marginalizing short wavelength fluctuations in higher-order terms is regarded as corrections to the coefficients in the Gaussian kernel.

Define $\big(\phi_p(\mathbf{q}),\phi_r(\mathbf{q})\big)^T=|\phi_{\mathbf{q}}\rangle$; also define a 2×2 matrix $\mathbf{M}(q)$ as:

$$\begin{array}{ll} M_{11}(q)=t+Kq^2+Lq^4, & M_{12}(q)=-m,\\ M_{21}(q)=-m^*, & M_{22}(q)=s,\end{array} \tag{84}$$

where $q=|\mathbf{q}|$. Then the Gaussian part of Hamiltonian in Eq. 25 can be written as:

$$\begin{aligned} -\beta\mathcal{H}_0 &= \int_0^\Lambda \frac{d^d\mathbf{q}}{(2\pi)^d}\,\frac{1}{2}\times\langle\phi_{\mathbf{q}}|\mathbf{M}(q)|\phi_{\mathbf{q}}\rangle\\ &= \int_0^\Lambda \frac{d^d\mathbf{q}}{(2\pi)^d}\,\frac{1}{2}\times\langle\phi_{\mathbf{q}}|UD(q)U^\dagger|\phi_{\mathbf{q}}\rangle\\ &= \int_0^\Lambda \frac{d^d\mathbf{q}}{(2\pi)^d}\,\frac{1}{2}\times\langle\psi_{\mathbf{q}}|D(q)|\psi_{\mathbf{q}}\rangle, \end{aligned} \tag{85}$$

where $|\psi_{\mathbf{q}}\rangle = U^\dagger|\phi_{\mathbf{q}}\rangle$, consisting of two orthogonal modes: $|\psi_{\mathbf{q}}\rangle=\big(\psi_1(\mathbf{q}),\psi_2(\mathbf{q})\big)^T$. U (as a function of q) is a unitary matrix, and $D(q)$ is a diagonal matrix.

$$\begin{aligned} \phi_p(\mathbf{q}) &= \langle\mathbf{1}|\Pi_1 U|\psi_{\mathbf{q}}\rangle,\\ \phi_r(\mathbf{q}) &= \langle\mathbf{1}|\Pi_2 U|\psi_{\mathbf{q}}\rangle. \end{aligned} \tag{86}$$

Here Π_α is a a projection matrix, and $|\mathbf{1}\rangle=(1,1)^T$. Under this construction, the perturbation term $\mathcal{U}$ in Eq. 26 can be re-expressed with $\psi_1(\mathbf{q})$ and $\psi_2(\mathbf{q})$, which have the following property:

$$\langle\psi_\alpha(\mathbf{q})\psi_\beta(\mathbf{q}')\rangle_0=\frac{\delta_{\alpha,\beta}(2\pi)^d\delta^d(\mathbf{q}+\mathbf{q}')}{D_{\alpha\beta}(q)}. \tag{87}$$

The subscript 0 is used to indicate that the expectation values are taken with respect to the unperturbed (Gaussian) Hamiltonian $\mathcal{H}_0$. One should be aware that the two-point correlation function has different average when choosing different modes. After choosing a renormalization size sacle $b>1$, we can also divide all modes to two parts according to their wavelength:

$$\psi_\alpha(\mathbf{q})=\begin{cases}\tilde{\psi}_\alpha(\mathbf{q}), & 0\le\mathbf{q}\le\Lambda/b;\\ \sigma_\alpha(\mathbf{q}), & \Lambda/b<\mathbf{q}\le\Lambda.\end{cases} \tag{88}$$

After re-expressing $\mathcal{U}$, there will be a number of 4^{th}-order terms with various combinations of $\psi_1(\mathbf{q})$ and $\psi_2(\mathbf{q}')$ to be averaged out with respect the Gaussian Hamiltonian associated with the short wavelength fluctuations:

$$\begin{aligned} &\big\langle\mathcal{U}[\vec{\tilde{\psi}},\vec{\sigma}]\big\rangle_\sigma=\sum_{\alpha,\beta,\gamma,\delta}C_{\alpha\beta\gamma\delta}\int_0^\Lambda\frac{d^d\mathbf{q_1}d^d\mathbf{q_2}d^d\mathbf{q_3}d^d\mathbf{q_4}}{(2\pi)^{4d}}\\ &(2\pi)^d\delta^d(\mathbf{q_1}+\mathbf{q_2}+\mathbf{q_3}+\mathbf{q_4})\cdot G_{\alpha\beta\gamma\delta}(q_1,q_2,q_3,q_4)\\ &\Big\langle\big[\tilde{\psi}_\alpha(\mathbf{q_1})+\sigma_\alpha(\mathbf{q_1})\big]\cdot\big[\tilde{\psi}_\beta(\mathbf{q_2})+\sigma_\beta(\mathbf{q_2})\big]\\ &\cdot\big[\tilde{\psi}_\gamma(\mathbf{q_3})+\sigma_\gamma(\mathbf{q_3})\big]\cdot\big[\tilde{\psi}_\delta(\mathbf{q_4})+\sigma_\delta(\mathbf{q_4})\big]\Big\rangle_\sigma. \end{aligned} \tag{89}$$

In this expression, $\alpha,\beta,\gamma,\delta=1,2$, and this summation goes over all non-repetitive combinations. $C_{\alpha\beta\gamma\delta}$ is a parameter that involves u, v, w, and some symmetry factor. $G_{\alpha\beta\gamma\delta}$ is a parameter that involves a bunch of $|\mathbf{q}|$ due to the fact that the inverse transformation in Eq. 86 is performed via a $\mathbf{q}$ "sensitive" unitary matrix U.

One should in principle to perform pair-wise contraction based onWick's theorem. However, there will be tremendous simplification when going into diagrammatic representation. In diagrammatic representation, to the p^{th} order in u, v, and w, a valid graph should have p vertices, four legs of each with internal momenta and indices (mode #ID) labeled by $(\mathbf{k}_i,\alpha_i)$, $i=1,2,3,4$, $\alpha=1,2$. One to four legs in each vertex should be replaced with "wires", representing a short wavelength σ mode. There should be two types of "wires" available to be drawn, since there are two modes of two-point correlation functions. Points connected with the same type of "wires" should be further jointed together with the same "wire". When calculating cumulants, only fully connected diagrams (without disjoint pieces or disobey of momentum conservation) need to be included.

After performing contraction and σ-mode integration in Eq. 89, we only keep on tracking those terms with one $\tilde{\psi}$-mode integration left, which adding-up together to the order of $p=1$ should has the form like:

$$\begin{aligned} &\sum_{\alpha=1}^2\int_0^{\Lambda/b}\frac{d^d\mathbf{q}}{(2\pi)^d}A_\alpha(q)|\tilde{\psi}_\alpha(\mathbf{q})|^2\\ =&\sum_{\alpha=1}^2\int_0^{\Lambda/b}\frac{d^d\mathbf{q}}{(2\pi)^d}A_\alpha(q)\big|\langle\mathbf{1}|\Pi_\alpha U^\dagger|\phi_{\mathbf{q}}\rangle\big|^2\\ =&\sum_{\alpha,\beta=1}^2\int_0^{\Lambda/b}\frac{d^d\mathbf{q}}{(2\pi)^d}B_{\alpha\beta}(q)\cdot\phi_\alpha(\mathbf{q})\phi_\beta(-\mathbf{q}). \end{aligned} \tag{90}$$

Here we transform ψ back to ϕ field. Finally, we expand $B_{\alpha\beta}(q)$ as power of q series, and subtract $2\times$ of the corresponding coefficient from $M_{\alpha\beta}(q)$ that match the same power of q. Consequently, we obtain the coarse-grained Gaussian kernel $\tilde{\mathbf{M}}(q)$.

The following rescale and renormalize steps are the same as Eq. 27. After choosing invariant parameters, one can write down differential equations governing the evolution of those parameters under rescaling, and analyze the linear stability along different directions. Addtion-

ally, higher diagrams ($p > 1$) should be perturbly obtained following the same principle.

To sum up, I proposed a framework of perturbative RG of Gaussian model with two interacting fields. The key point is to orthogonalize two interacting fields before coarse-grain, and perform averaging over $\mathcal{U}$ with orthogonal short wavelength vectors (to get rid of fluctuation). Finally, orthogonal fields are back-transformed to the original interacting fields, and corrections to the coefficients in the Gaussian Kernel are paired in power of q.